

SECONDARY FLOW IN A TURBULENT
BOUNDARY LAYER¹

by

S. D. VEENHUIZEN* and R. N. MERONEY**

Fluid Dynamics and Diffusion Laboratory
Colorado State University

Submitted to

Journal of the Hydraulics Division
Proceedings of the American Society
of Civil Engineers

¹The authors gratefully acknowledge support for this work under DOD Contract No. N00014-68-A-0493-0001 (Project No. NR 062-414/6-6-68) (Code 438).

*Research Assistant, Colorado State University, Fort Collins, Colorado.

**Associate Professor, Department of Civil Engineering, Colorado State University, Fort Collins, Colorado.

ABSTRACT

The secondary flow in the developing boundary layer of a square duct is experimentally investigated. Measurements of the horizontal components of secondary flow were made for free stream velocities of 3, 6.1, and 12.2 m/s, corresponding to Reynolds numbers based on hydraulic diameter of 3.6×10^5 , 7.2×10^5 , and 1.4×10^6 at a ratio of L/D_h of 6.7. Measurements of the developing boundary layer parameters and turbulence quantities in a corner were made for the intermediate Reynolds number.

The secondary flow and turbulence distribution in a corner are discussed and compared with the fully developed flow situation. The results indicate the maximum secondary flow velocity is less than 2% of the free stream velocity, and that the secondary flow may encompass the entire cross section. The turbulence distribution was found to not differ fundamentally from those found in fully developed flow.

INTRODUCTION

A variety of fluid mechanic experiments have been performed in wind-tunnels with thick boundary layers. For example, studies of the action of wind on buildings in the atmospheric shear layer; instantaneous and continuous diffusion from line and point sources with a variety of stratification and roughness conditions and basic boundary layer research have been done. In most cases, the flow is assumed to be two-dimensional in nature. Unfortunately, turbulent flow in straight ducts of noncircular cross section is generally of a three-dimensional nature. The mean velocity vector consists of a primary component in the axial direction and a transverse component in the plane perpendicular to the axial direction. The turbulence properties of these flows are also generally of a three-dimensional nature. This study was instituted to evaluate perturbations generated by the background flow field which must be subtracted from effects directly related to three-dimensional nonhomogenetics in roughness or temperature.

The most obvious characteristic of this inherent three-dimensionality is the now commonly accepted distortion of the lines of constant velocity, or isovels, particularly in the region of a corner. Nikuradse (10) was the first to observe experimentally that the isovels were displaced toward the walls in corner regions and away from the walls at the mid-points between corners of a triangular duct. From this, Prandtl (14) concluded that a flow component must exist perpendicular to the isovels at points of nonuniform isovel curvature and be directed from the concave side to the convex side of an isovel. The effect of the transverse flow was to convect higher momentum fluid into the corner regions and lower momentum fluid into the center region of the duct at mid-points

between corners. These transverse currents have since become known as secondary flows and are generally regarded as superimposed upon the axial mean flow.

Since the time of Nikuradse's and of Prandtl's initial exploration, conclusive experimental information regarding secondary flow awaited the innovation of the hot-wire anemometer. Several discussions of an analytic nature were also advanced. Maslen (9) was able to show that secondary flows could not generate themselves in a fully developed laminar flow, and Einstein and Li (3) were able to indicate that gradients in the turbulent stresses were responsible for generation of secondary flow in fully developed turbulent flows. Earlier, Townsend (16) had suggested that the cross currents were the result of gradients in the wall shear stress.

Hoagland (6) was the first to actually measure the magnitude of the secondary flow components in a closed, noncircular duct with fully developed flow. Gessner (5), and Brundrett and Baines (1) expanded the investigation of fully developed flow in closed square ducts. (Gessner (5) and Tracy (17) also examined rectangular ducts.) Experimental investigation of the secondary flow in the entrance region of a closed duct, where the flow was not fully developed, was initiated by Pletcher and McManus (13). Perkins (11) also reported a series of measurements made in a developing flow field; however, he only reported detailed results for the near-corner region.

With the exception of the study performed by Pletcher and McManus, and Perkins in the entrance region of a rectangular duct, the previous studies of secondary flows have been restricted to the fully developed flow case. The present investigation is intended to examine further

the case of a developing turbulent flow, in particular, the boundary layer developing along the floor of a wind tunnel with the emphasis placed on experimentally determining the regions of secondary flow.

ANALYTICAL BACKGROUND

The equations governing a general flow are the turbulent Navier-Stokes equations of motion and the equation of continuity. Under the restrictions of steady and incompressible flow, the momentum equation is in tensor notation

$$\rho U_j \frac{\partial U_i}{\partial x_j} = - \frac{\partial P}{\partial x_i} + \mu \frac{\partial^2 U_i}{\partial x_j \partial x_j} - \rho \frac{\partial}{\partial x_j} (\overline{u_i u_j}) \quad (1)$$

for $i, j = 1, 2, \text{ and } 3$. The U_i are the mean velocities in the three coordinate directions, the subscript 1 denoting the axial, with 2 denoting the vertical, and 3 the horizontal direction. The last term in equation (1) is the apparent Reynold's stresses. The other symbols have their standard meanings.

The continuity equation for the mean flow is

$$\frac{\partial U_i}{\partial x_i} = 0 \quad (2)$$

and for the turbulent components is

$$\frac{\partial u_i}{\partial x_i} = 0 \quad (3)$$

Operating on equation (1) with the curl operator, and manipulating with the continuity equations, produces the vorticity equation. It is

$$\rho U_k \frac{\partial \Omega_\ell}{\partial x_k} - \rho \Omega_k \frac{\partial U_\ell}{\partial x_k} = \epsilon_{jil} \frac{\partial}{\partial x_j \partial x_k} (-\rho \overline{u_i u_k}) + \mu \frac{\partial^2 \Omega_\ell}{\partial x_k \partial x_k} \quad (4)$$

where $\Omega_\ell = \epsilon_{jil} \frac{\partial U_i}{\partial x_j}$ is the mean vorticity vector about the ℓ direction and ϵ_{jil} is the alternating third order permutation tensor.

When the flow is fully developed some simplification of the governing equations is possible. Fully developed flow is taken to mean all variables are constant in the axial, or mean flow direction, i.e., derivatives with respect to x_1 are zero. With this simplification introduced, the axial momentum equation is

$$\rho U_2 \frac{\partial U_1}{\partial x_2} + \rho U_3 \frac{\partial U_1}{\partial x_3} = - \frac{\partial P}{\partial x_1} + \mu \left(\frac{\partial^2 U_1}{\partial x_2^2} + \frac{\partial^2 U_1}{\partial x_3^2} \right) - \rho \frac{\partial}{\partial x_2} (\overline{u_1 u_2}) - \rho \frac{\partial}{\partial x_3} (\overline{u_1 u_3}) \quad (5)$$

The continuity equations are written as

$$\frac{\partial U_2}{\partial x_2} + \frac{\partial U_3}{\partial x_3} = 0 \quad (6)$$

and

$$\frac{\partial u_2}{\partial x_2} + \frac{\partial u_3}{\partial x_3} = 0 \quad (7)$$

Analytic solutions of these equations appear to be as unapproachable as solutions to the full equations. Liggett, Chiu and Miao (7) used a semi-theoretical approach, wherein the axial equation of motion was transformed into an equation in coordinates corresponding to the isovels of the mean axial flow and their perpendiculars. The measured axial mean velocity profiles were used with von Karman's equation for shear in a finite difference form of the transformed equation of motion to obtain a numerical solution for the flow in a 90° corner. The results obtained did compare favorably with experimental measurements for a 90° "V" open channel.

The vorticity equation for fully developed flow has been discussed extensively by Brundrett and Baines (1) and Einstein and Li (3). With the above mentioned simplification for fully developed flow, vorticity equation for the axial vorticity is

$$U_2 \frac{\partial \Omega_1}{\partial x_2} + U_3 \frac{\partial \Omega_1}{\partial x_3} = \frac{\partial^2}{\partial x_2 \partial x_3} (\overline{u_3^2} - \overline{u_2^2}) - \left(\frac{\partial^2}{\partial x_2^2} - \frac{\partial^2}{\partial x_3^2} \right) \overline{u_2 u_3} + v \left(\frac{\partial^2 \Omega_1}{\partial x_2^2} + \frac{\partial^2 \Omega_1}{\partial x_3^2} \right) . \quad (8)$$

The terms on the right, involving the fluctuating components of velocity, are commonly thought of as the source of vorticity production.

If $U_2 = U_3 = 0$, there is no secondary flow by definition, and there is no axial vorticity, since $\Omega_1 = \partial U_3 / \partial x_2 - \partial U_2 / \partial x_3$. Conversely, when $\Omega_1 = 0$, U_2 and U_3 can be shown to satisfy Laplace's two dimensional equation and must be zero since $U_2 = U_3 = 0$ on the boundaries. In either case, the terms involving the mean quantities in equation (8) reduces to zero, resulting in

$$\frac{\partial^2}{\partial x_2 \partial x_3} (\overline{u_3^2} - \overline{u_2^2}) - \left(\frac{\partial^2}{\partial x_2^2} - \frac{\partial^2}{\partial x_3^2} \right) \overline{u_2 u_3} = 0 . \quad (9)$$

When the terms of equation (9) make a non-zero contribution, vorticity exists, thus the terms of equation (9) are termed vorticity production terms.

The developing flow found in the entrance regions of non-circular wind tunnels is characterized by two regions of flow; the free stream, and the boundary layers which develop along the walls. The entrance conditions greatly influence the characteristics of the flow in the free stream, and to a lesser extent, in the boundary layers. The

turbulence characteristics of the free stream are dependent upon the characteristics of the fluid before it enters the duct, and it also depends upon the physical structures which are located in the entrance. Although correlations between the entrance conditions and the turbulence characteristics directly downstream have been studied it has never been determined how to relate them to solutions of the flow field. The entrance conditions at the beginning of the boundary layer affect the turbulence characteristics of the flow field for some distance downstream, although, at sufficient distances from the beginning these effects decay and the boundary layer approaches an equilibrium boundary layer.

Interaction between the free stream and the outer edges of the boundary layer creates further complications. Intermittency of turbulence is a characteristic of this interaction between the two regions of flow. Little is actually known about this intermittency except that it is dependent upon the free stream turbulence level and upon the external pressure gradient of the free stream.

The mathematical description of secondary flow in a three-dimensional boundary layer becomes more cumbersome because the axial derivatives do not reduce to zero. Boundary layer approximations to reduce the complexity of the equations of motion are not applicable, since these approximations generally assume the flow field to be of a two-dimensional nature. Three-dimensional boundary layer equations have been developed by Mager (8) and Sears (15), but these apply specifically to the region of the boundary layer. Introducing secondary flow of this nature into the boundary layer equations would require modification of the boundary conditions of the external boundary. This modification would take the form of making these conditions functional in nature. As such, they

they would become part of the solution to be solved for, thereby increasing the complexity of the solution.

The equation for the axial vorticity without the previous simplification now contains all of its terms

$$\begin{aligned}
 U_1 \frac{\partial \Omega_1}{\partial x_1} + U_2 \frac{\partial \Omega_1}{\partial x_2} + U_3 \frac{\partial \Omega_1}{\partial x_3} - \Omega_1 \frac{\partial U_1}{\partial x_1} - \Omega_2 \frac{\partial U_1}{\partial x_2} - \Omega_3 \frac{\partial U_1}{\partial x_3} = \nabla^2 \Omega_1 \\
 + \frac{\partial^2}{\partial x_2 \partial x_3} (\overline{u_3^2} - \overline{u_3^2}) - \left(\frac{\partial^2}{\partial x_2^2} - \frac{\partial^2}{\partial x_3^2} \right) \overline{u_2 u_3} \\
 + \frac{\partial^2}{\partial x_1 \partial x_3} (\overline{u_1 u_2}) - \frac{\partial^2}{\partial x_1 \partial x_2} (\overline{u_1 u_3})
 \end{aligned} \tag{10}$$

where ∇^2 is the usual Laplacian. In addition to the equations for mean vorticity in the three coordinate directions, a continuity equation for vorticity is available. It is

$$\frac{\partial \Omega_1}{\partial x_1} + \frac{\partial \Omega_2}{\partial x_2} + \frac{\partial \Omega_3}{\partial x_3} = 0 \tag{11}$$

Solutions to the equations for a developing flow do not appear any more accessible than the fully developed flow equations.

EXPERIMENTAL EQUATIONS AND PROCEDURES

The U. S. Army Micrometeorological wind tunnel, Figure 1 was designed to simulate atmospheric boundary layer effects. The test section of approximately 30 meters in length and a 2 meter by 2 meter cross section constituted one side of the recirculating system with the driving motor and heating-cooling coils located on the opposite side. From the stilling chamber the air passed through four fine-mesh screens with a wire diameter of 0.19 millimeters, and 9.45 by 9.45 meshes-per square centimeter, followed by a nine to one contraction down to the test

section entrance. Around the test section entrance was a gravel roughness 1.3 centimeters high and 1.2 meters in length, followed by a 3.8 centimeter high sawtooth fence used to trip the boundary layer. A complete description of this facility is given by Plate and Cermak (12).

For secondary flow measurements, a rotating constant temperature hot-wire anemometer technique, similar to that used by Hoagland (6), Gessner (5), and Brundrett and Baines (1), was utilized. This technique employs the following physical characteristic of the hot wire: When a hot wire, operating at constant temperature, is parallel to the flow direction, a minimum heat loss from the wire to the fluid occurs, and therefore, a minimum voltage output is obtained. Yawing of the wire about the position where the wire is parallel to the flow direction produces, for a well constructed hot wire, a voltage signal which is symmetrical about the flow direction. To determine the flow direction, the hot wire is rotated either clockwise, or counterclockwise, about an axis that is normal (usually the probe axis) to the wire axis, until the wire is yawed approximately twenty degrees from the direction of flow and the wire signal noted. Rotation of the wire in the opposite direction, until the noted signal is again obtained, will determine the flow direction as being half the total angular change from one position to the other. Accuracy of the method is limited by the turbulence level of the fluid passing by the wire (2) and by the ability to determine the angular position of the hot wire itself. Accuracy under the present conditions was ± 0.05 degrees for any single realization.

The following method of probe alignment was used to measure the flow direction, from which the horizontal components of the total velocity vector were calculated. The free stream direction in the tunnel was used as the reference direction for determining the reference position of the hot wire probe. This reference was used since preliminary measurements in the free stream of the tunnel indicated that the free stream direction coincided with the geometrical center line of the tunnel.

Alignment of the hot wire was accomplished by employing a reference line fixed to the base of the stand on which the rotating hot wire and its rotating mechanism were mounted. The reference line was then oriented in the free stream with a transit aligned with the tunnel. This procedure yielded the relationship between the reference line, the center line of the tunnel, and the hot wire and allowed re-alignment at any position in the cross section of the tunnel. The hot wire filament used for these measurements was a platinum wire 10.2 microns in diameter and 13 millimeters in length, mounted on a probe with prongs 2.6 centimeters in length.

For the determination of the mean velocity profiles and the longitudinal turbulence intensity a single hot wire was used normal to the flow in a horizontal position. The wire used was a 5.1 micron diameter tungsten wire approximately 2.5 millimeters in length. An x-wire probe was used for the measurement of Reynolds' stresses. Considerable effort was expended to orient the wires at right angles to each other. The hot wires were operated with Colorado State University Constant Temperature Anemometers, model HW300B (4). The root-mean-square values were recorded from a B and K, model 2409 true RMS meter.

A pitot static probe type PAC-12-KL from United Sensor and Control Corporation was used in conjunction with a Transonics Equibar Type 120 electronic manometer to monitor the free stream velocity and to make several velocity profile surveys. The hot wires described above were calibrated using the pitot tube as a standard. The calibrations were performed in free stream of the wind tunnel where there was a minimum turbulence level.

Only horizontal components of the secondary flow were measured using the long, single rotating wire in the test quadrant. The quadrant studied was the lower right quadrant of the cross section when observing it in the stream-wise direction, located 12 meters from the sawtooth roughness at the entrance. The cross section of the tunnel had a hydraulic diameter of 1.8 meters, giving a L/D_h ratio of 6.7. The range of Reynolds numbers based on the free stream speed and the hydraulic diameter was from 3.6×10^5 to 1.4×10^6 .

EXPERIMENTAL RESULTS AND DISCUSSION

Several boundary layer parameters--boundary layer thickness, displacement thickness, momentum thickness, and shape factor--were determined from a series of velocity profiles on the center line of the test section at several stations from the entrance. Figure 2 shows the velocity profiles plotted in non-dimensional form. The boundary layer parameters, shown in figure 3, are indicative of a zero pressure gradient boundary layer which has a constant shape factor and constant wall shear after some distance downstream of the entrance.

Profiles of mean velocity in the cross section 12 meters from the entrance indicate the flow is not symmetrical with respect to the

center of the cross section. There are two aspects of the nonsymmetrical behavior. First, as indicated by the isovels for the test quadrant figure 4, the mean motion is displaced approximately six to eight centimeters from the center line of the test section. It appears that this condition existed throughout the length of the test section. Secondly, the boundary layers on the tunnel boundaries grew at different rates. That is, as figure 4 shows, the boundary layers on the vertical walls were not as thick as the one along the flow.

The isovels of figure 4 show the same penetration into the corner and displacement from the wall at the center line as is characteristics of a fully developed duct flow. As pointed out below, this has particular significance.

The mean transverse velocities measured in the horizontal plane are shown in figures 5 and 6. In figure 5 the ordinate has been nondimensionalized with the boundary layer thickness at the center line, and in figure 6 with the half height of the tunnel cross section. The data shown, collapses better, in general, using the boundary layer thickness for nondimensionalizing the vertical coordinates, however, the data in the corner collapses better if the half height is used in place of the boundary layer thickness. This implies that the flow distribution away from the corner is influenced more by the boundary layers, whereas in the corner, it is influenced more by the geometry of the corner. From these measurements approximate values were obtained for the vertical components of the secondary flow.

To obtain values of the vertical component, the continuity equation was integrated graphically:

$$U_2(x_2) = - \int_0^{x_2} \left(\frac{\partial U_1}{\partial x_1} + \frac{\partial U_3}{\partial x_3} \right) d\eta + F(x_1) + G(x_3) \quad (12)$$

where $F(x_1) = G(x_3) = 0$. The term $\partial U_3 / \partial x_3$ was obtained graphically from the measured values for U_3 . An estimation of an average value for $\partial U_1 / \partial x_1$ was obtained by differentiating the displacement thickness, with respect to x_1 , to obtain

$$\frac{\partial U_1}{\partial x_1} = \frac{U_\infty}{\delta} \frac{\partial \delta_*}{\partial x_1} \quad (13)$$

Thus, equation (9) becomes

$$U_2(x_2) = - \int_0^{x_2} \frac{\partial U_3}{\partial x_3} d\eta + \frac{U_\infty}{\delta} \frac{\partial \delta_*}{\partial x_1} x_2 \quad (14)$$

which was used to calculate the vertical component of the secondary flow shown in figure 7. Of the two terms on the right side of equation (14), the first is at least one order of magnitude, or more larger than the second. Near the center of the cross section is the region of upward flow characteristic of a developing boundary layer and of secondary flows. In the corner, is the region of downward flow characteristic of secondary flow. These two regions agree with Prandtl's prediction of secondary flow direction based on isovels exhibited for fully developed duct flow. The same is true for boundary layer flows, that is, the secondary flow direction is from the concave to the convex side of an isovel. The relatively strong positive vertical component at $x_3/d_3 = 0.55$ is not clearly understood. A possible explanation for it may be that there is more than one secondary flow pattern present in the part of the boundary layer as suggested by Pletcher and McManus (13) and Perkins (11).

A comparison of data from this experiment, with selected data from previous experiments of other investigators, is given in figure 8. The data from Pletcher and McManus is for fully developed flow, as are the data shown from other investigators; however, the Pletcher and McManus data is from a 3:1 aspect ratio duct. The coordinates for this data were nondimensionalized, using the half width for the minor dimension. The bottom portion of figure 8 indicates that the present data have a definite shift in the direction of increased flow away from the vertical wall, compared to previous information. The same is true in the upper part of figure 8, for the upper half of the data, but as the floor is approached, the agreement between the present data and previous data becomes better. The large discrepancy in the upper part of the figure may be due to the relative influence of the corner geometry and the boundary layers. The fact that the boundary layer along the vertical wall differed from that along the floor may also contribute significantly to this discrepancy. A significant fact worthy of note is the effect of using the boundary layer thickness in place of the half height for making the ordinate dimensionless. For the fully developed flow data shown, no change would occur since the boundary layer thickness would be equivalent to the half height. The data from the developing boundary layer would change significantly. The boundary layer thickness was approximately half, or less of the half height of the tunnel which would move the data from this experiment out of the range of the fully developed flow data.

The resultants of the measured mean horizontal components and the calculated vertical components are shown in figures 9, 10, and 11, for three different free stream speeds. The flow in the corner, along the vertical wall, and along the floor, was similar for all three speeds.

In the area nearer the center of the cross section, the resultants for the lower speed exhibit a direction opposite to those in the same relative position for the two higher speeds. The absolute value of the secondary velocities in the area were very small, indicating weak secondary currents. In comparing the lower speed resultants with the two higher speed resultants, suspicion arises that the flow has not developed sufficiently to establish the secondary currents. Of note is that the measured secondary flows are all less than two percent of the free stream speed which agrees with the results for fully developed flows.

In considering fully developed flows the introduction of a stream function for the secondary currents through the continuity equation will result in what is called a secondary flow cell. In a particular cross section the stream lines must close on themselves since the flow away from a boundary must equal the flow toward the boundary. The same concept may be applied to the developing flow; however, it will not necessarily have the characteristic of the stream lines closing upon themselves in a particular cross section since the rate of fluid flow in the axial direction may change in the axial direction for a developing boundary layer. Even with this distinction the word cell is attractive to describe the patterns of secondary flow. The velocity resultants shown in figures 9, 10, and 11 indicate at least two regions of the cross section where the fluid is rotating about a longitudinal axis. If cells were to be constructed from the velocity resultants shown, it is apparent that, if nearly closed cells are imagined to exist, they must be completed outside the boundary layers. Otherwise a return flow from the center line to the wall would have been observed within the boundary layer. That is, the cell would encompass not only the boundary

layers, but the free stream as well. Whether or not the free stream actually has transverse currents was not determined in this experiment, however, Pletcher and McManus indicate secondary flow velocities along the axis of symmetry for their cross section in the entrance region of their duct. If such currents do exist, the concept of a potential core will need some alteration. Obviously such secondary flows in the free stream are the result of only advection and any vorticity generation must occur within the boundary layer.

The turbulent stresses were measured in the same cross section as the secondary flow component for the intermediate free stream speed of 6.1 meters per second, with the exception of $\overline{u_2 u_3}$. Figures 12, 13, and 14 display the distribution of the normal intensities in the cross section. Shown are contours which were interpolated between values determined at a number of grid points in the cross section. Of note is the penetration of the contours into the corner along the corner bisector (CB) characteristic of turbulent flow along a corner. The penetration appears to be more severe than for fully developed turbulent flow, due to the possible convection of fluid from the free stream containing little turbulence energy. The turbulence level in the free stream of the test facility was below 0.02%. The departure of the contours from the wall in the region of the center line is indicative of the secondary flow at the center line, similar to the isovels in figure 4.

The distribution in the cross section of the difference $(\overline{u_3^2} - \overline{u_2^2})$ is shown in figure 15. The mixed second derivative, with respect to x_2 and x_3 of this difference is the vorticity production term of equation (7). This second derivative was not evaluated because of the uncertainty

in obtaining a second derivative from experimental data, but from the distribution shown, the magnitude of the production term is greater along the wall than along the floor indicating stronger vorticity along the wall. This agrees with the resultant velocities of figure 9, 10, and 11 in the same region.

Figures 16 and 17 show the distributions of the turbulent shear terms in the cross section. Again, these are characteristic of flow along a corner with secondary flow. It is the derivatives of the cross gradients of these terms, with respect to x_1 , that indicate a transfer of vorticity from the lateral directions into the axial direction in a developing flow.

CONCLUSION

The general pattern of secondary flow in a developing boundary layer, as implied by the experimental data shown in the figures, is one in which a cross flow along the tunnel floor occurs from the wall to the center line of the cross section. At the center line the cross flow turns upward along the bisector of the floor boundary and appears to continue through the boundary layer into the free stream. Thus, low momentum fluid is convected from the corners, across the boundary layer along the floor to the center of the cross section, and up into the free stream along the vertical axis of symmetry of the duct.

A flow from the free stream into the corner occurs along the corner bisector. Of particular interest is the observation that no measurements indicated a flow from the center of the duct to the corners within the boundary layer along the floor. Along the vertical wall such a flow was indicated.

The strength of the secondary currents may be influenced by an interaction of the relative boundary layer thicknesses and the geometry of the corner. The two effects can not be separated; however, immediately at the corner the geometry of the corner predominates. In all cases the maximum measured secondary flow velocity magnitude was less than two percent of the free stream speed.

Whether or not the cross currents connect the free stream and boundary layer is speculative, based on the experimental evidence presented here. The term responsible for the production of vorticity does not exist in the free stream of this study, thus, the vorticity can only be dissipated in the free stream, not strengthened.

Associated with the pattern of secondary motion is the distribution of the turbulence stresses. The distributions measured differ from those of fully developed turbulent duct flow in that all approach zero magnitude near the edge of the boundary layer and remain zero throughout the free stream region of flow. Otherwise the distribution in the cross section is quite similar to fully developed turbulent flow along a corner.

REFERENCES

1. Brundrett, E. and Baines, W. D., The Production and Diffusion of Vorticity of Duct Flow, *Journal of Fluid Mechanics*, 19, (1964), 375.
2. Delleur, J. W., Flow Direction Measurement with Hot Wire Anemometers. Presented at the Hydraulics Division Conference, ASCE, Tucson, Arizona, (August 25, 1965).
3. Einstein, H. A. and Li, H., Secondary Currents in Straight Channels, *American Geophysical Union, Trans.*, 39, No. 6, (December 1958).
4. Finn, C. L. and Sandborn, V. A., Design of a Constant Temperature Hot-Wire Anemometer. U. S. Army Grant DA-AMC-28-043-65-G20, NASA, NGR-06-002-038, CER66-67CLF36, Colorado State University, Fort Collins, (March 1967).
5. Gessner, F. B., Turbulence and Mean-Flow Characteristics of Fully Developed Flow in Rectangular Channel. Ph.D. dissertation, Purdue University, (January 1964). (Also see *Journal of Fluid Mechanics*, 23, (1965), 689.)
6. Hoagland, L. C., Fully Developed Turbulent Flow in Straight Rectangular Ducts - Secondary Flow; Its Cause and Effect on the Primary Flow. Ph.D. dissertation, Massachusetts Institute of Technology, (1960).
7. Liggett, J. A., Chiu, C. L. and Miao, L. S., Secondary Currents in a Corner, *Journal of the Hydraulics Division, ASCE*, 91, (1965).
8. Mager, A., Generalization of Boundary Layer Momentum-Integral Equations to Three Dimensional Flow Including Those of a Rotating System, NACA Report 1067, (1952).
9. Maslen, S. H., Transverse Velocities in Fully Developed Flows, *Quarterly Journal of Applied Mathematics*, 16, (1958), 173.

10. Nikuradse, J., Untersuchungen über die Geschwindigkeitsverteilung in Turbulenten Stromungen, VDI-Forschungsheft 281, Berlin (1926).
11. Perkins, H. J., The Formation of Streamwise Vorticity in Turbulent Flow. Cambridge University Department of Engineering - Report CUED/A-Turbo/T.R.6 (1969).
12. Plate, E. J. and Cermak, J. E., Micro-Meteorological Wind Tunnel Facility. Final Report, Fluid Dynamics and Diffusion Laboratory, Colorado State University, CER63EJP-JEC9, (February 1963).
13. Pletcher, R. H. and McManus, H. N., Secondary Flow in the Entrance Section of a Straight Rectangular Duct, Proc. 8th Mid-Western Conference on Mechanics, (1963).
14. Prandtl, L., Über die ausgebildete Turbulenz, Verhandlungen des zweiten Internationalen Kongresses für Technische Mechanik, Zurich, (1926).
15. Sears, W. R., Boundary Layers in Three-Dimensional Flow, Applied Mechanics Review, 7, (1954), 281.
16. Townsend, A. A., The Structure of Turbulent Shear Flow. University Press, Cambridge, (1956).
17. Tracy, H. J., Turbulent Flow in a Three-Dimensional Channel, Journal of the Hydraulics Division, ASCE, 91, (1965), 9.

LIST OF SYMBOLS

<u>Symbol</u>	<u>Definition</u>	<u>Dimensions</u>
D_h	Hydraulic diameter	L
d_i	Half width, height of tunnel cross section	L
H	Shape factor	
i	Index	
j	Index	
k	Index	
L	Wind tunnel width	L
l	Index	
P	Mean pressure	ML/T ²
U_i	Mean velocity in i-th direction	L/T
$U_{i,j}$	Resultant of i-th and j-th mean velocity components	L/T
U_∞	Free stream velocity	L/T
u_i	Turbulent velocity component in i-th direction	L/T
$\overline{u_i u_j}$	Time mean of product of u_i and u_j	L ² /T ²
x_i	Spatial coordinate in i-th direction	L
δ	Boundary layer thickness along centerline	L
δ	Displacement thickness	L
ϵ_{ijk}	Alternating third order permutation tensor	
η	Variable of integration	L
θ	Momentum thickness	L
μ	Dynamic viscosity	M/LT
ν	Kinematic viscosity	L ² /T
ρ	Density	M/L ³
Ω_i	Mean vorticity about i-th direction	1/T

LIST OF FIGURES

Fig. No.

1. Wind Tunnel
2. Velocity profiles along centerline of wind tunnel
3. Boundary layer parameters
4. Isovels
5. Horizontal secondary flow components; U_3/U_∞ vs x_2/δ
6. Horizontal secondary flow components; U_3/U_∞ vs x_2/d_2
7. Calculated vertical secondary flow components; U_2/U_∞ vs x_3/d_3
8. Comparison with data of other investigators
9. Resultant secondary flow in cross section, $U_\infty = 3$ m/s
10. Resultant secondary flow in cross section, $U_\infty = 6.1$ m/s
11. Resultant secondary flow in cross section, $U_\infty = 12.2$ m/s
12. Distribution of $\overline{u_1^2}/U_\infty^2$
13. Distribution of $\overline{u_2^2}/U_\infty^2$
14. Distribution of $\overline{u_3^2}/U_\infty^2$
15. Distribution of $(\overline{u_3^2} - \overline{u_2^2})/U_\infty^2$
16. Distribution of $\overline{u_1 u_2}/U_\infty^2$
17. Distribution of $\overline{u_1 u_3}/U_\infty^2$

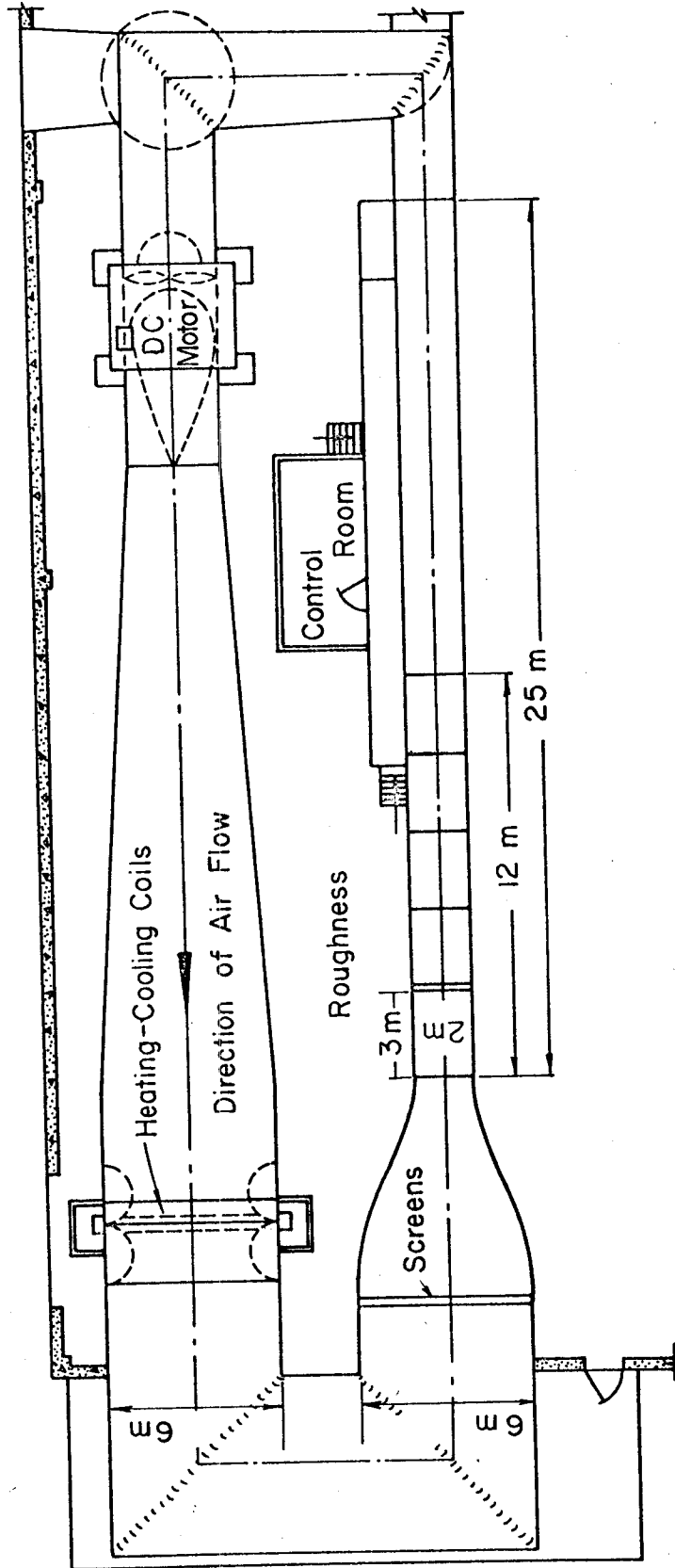


Fig. 1. Wind tunnel

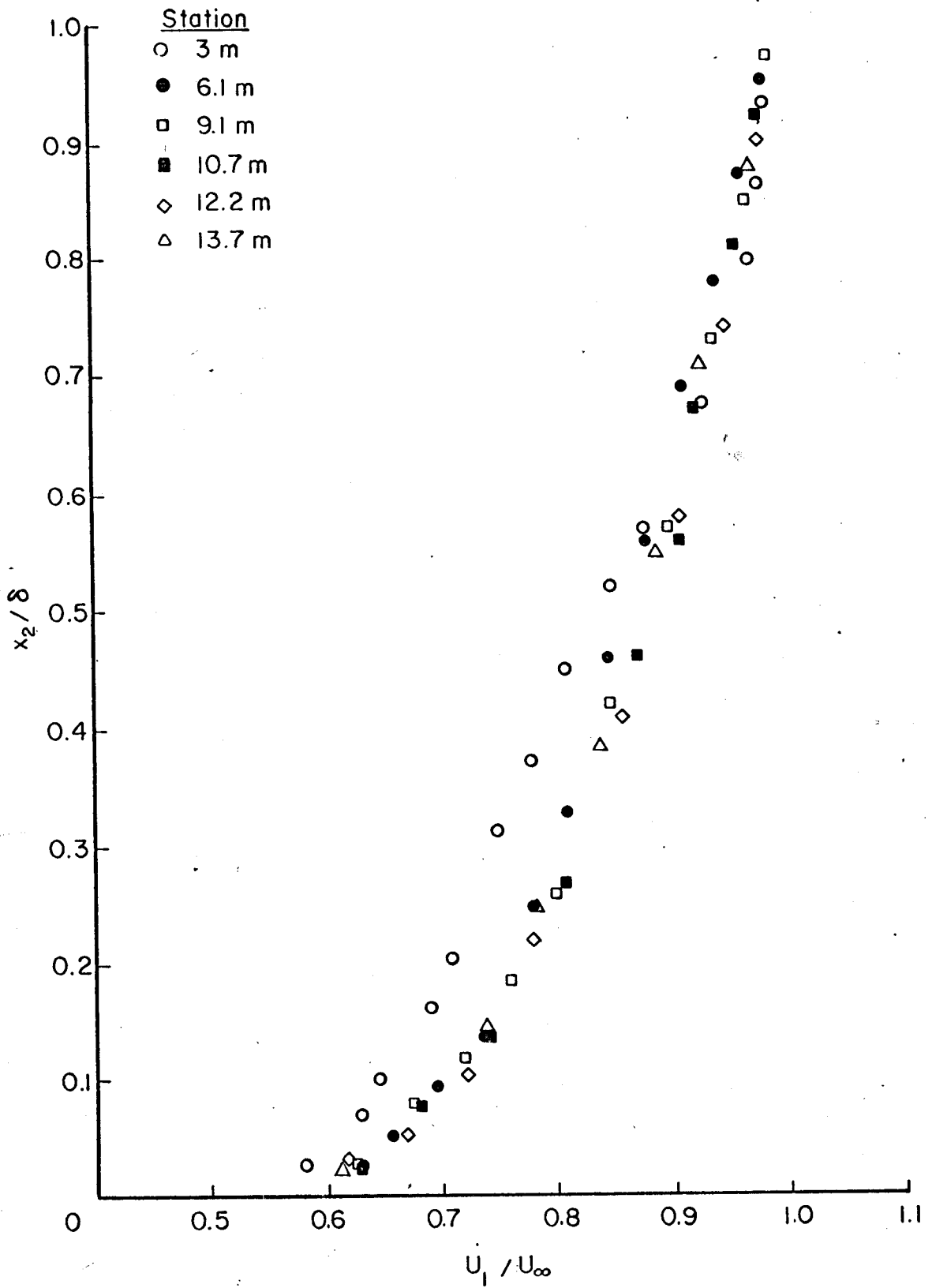


Fig. 2. Velocity profiles along centerline of wind tunnel

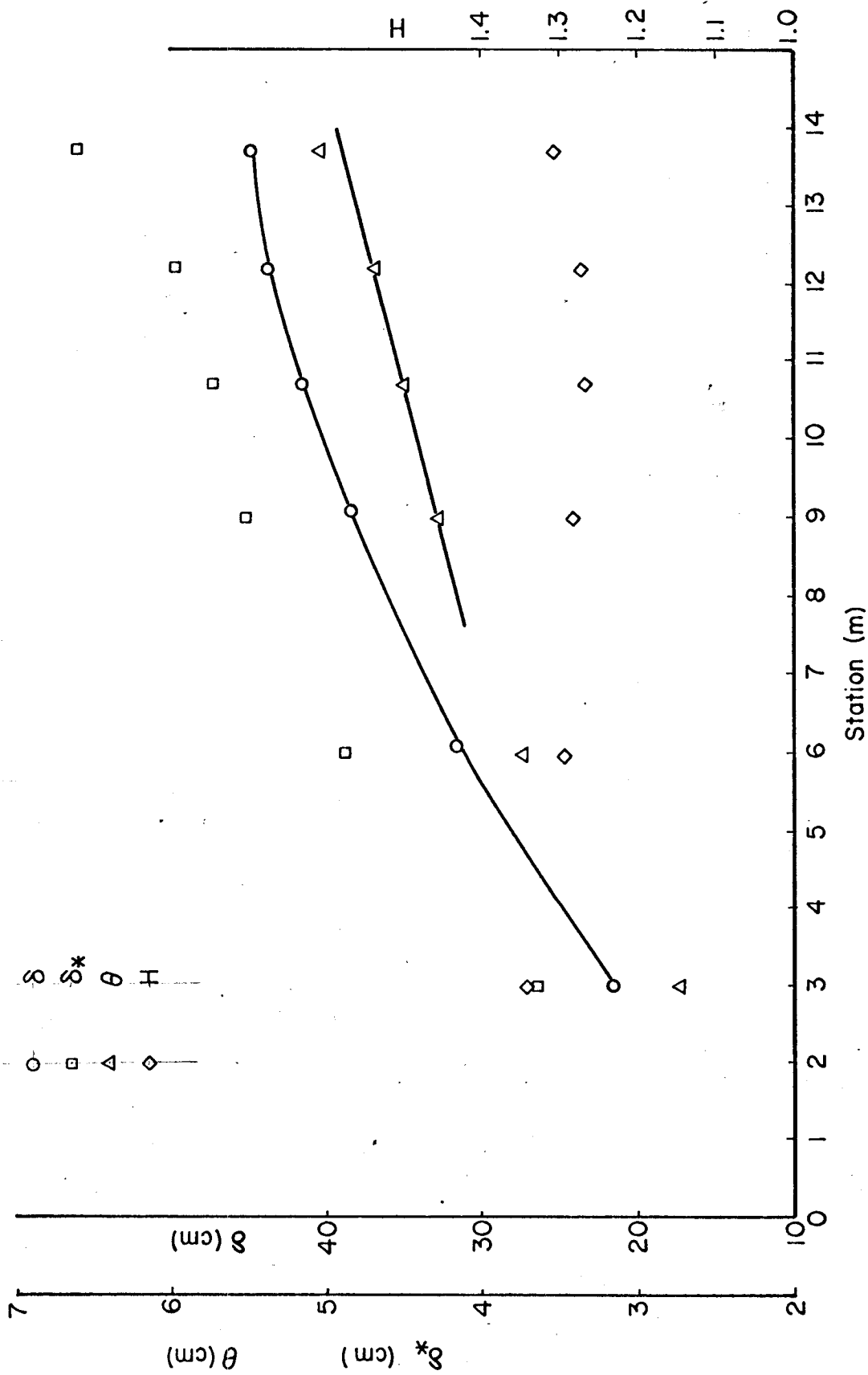


Fig. 3. Boundary layer parameters

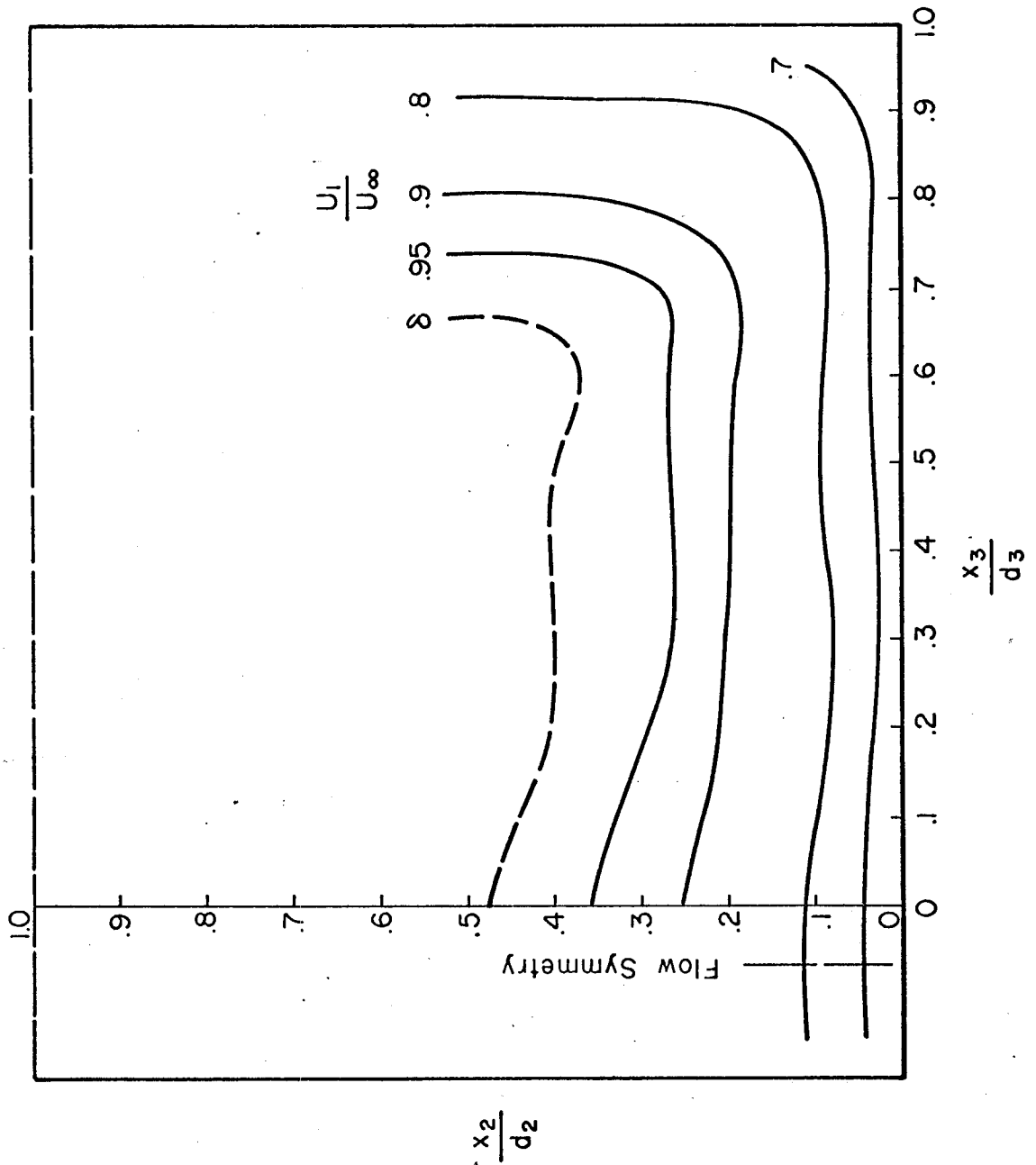


Fig. 4. Isovels

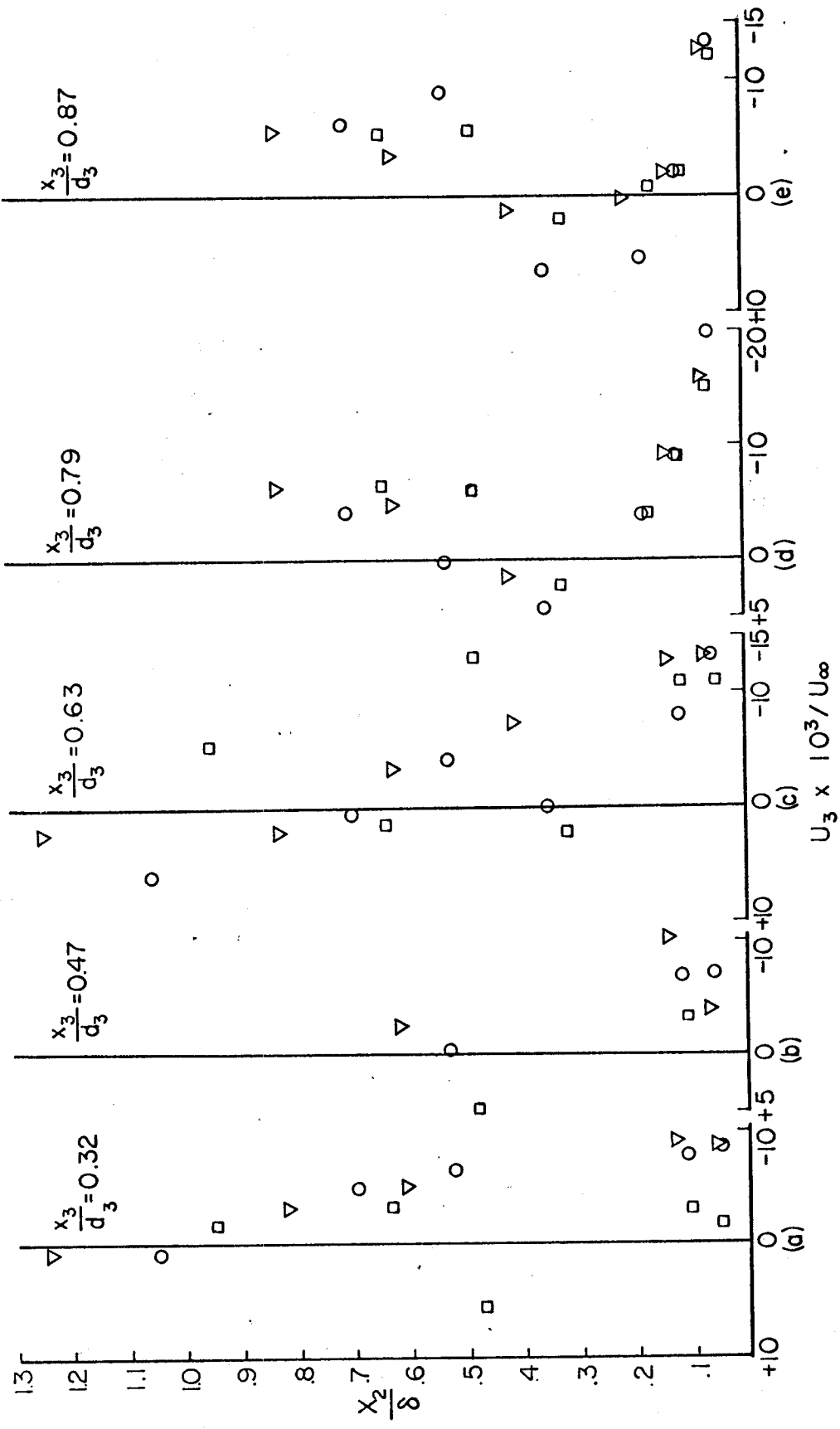


Fig. 5. Horizontal secondary flow components: U_3/U_∞ vs x_2/δ

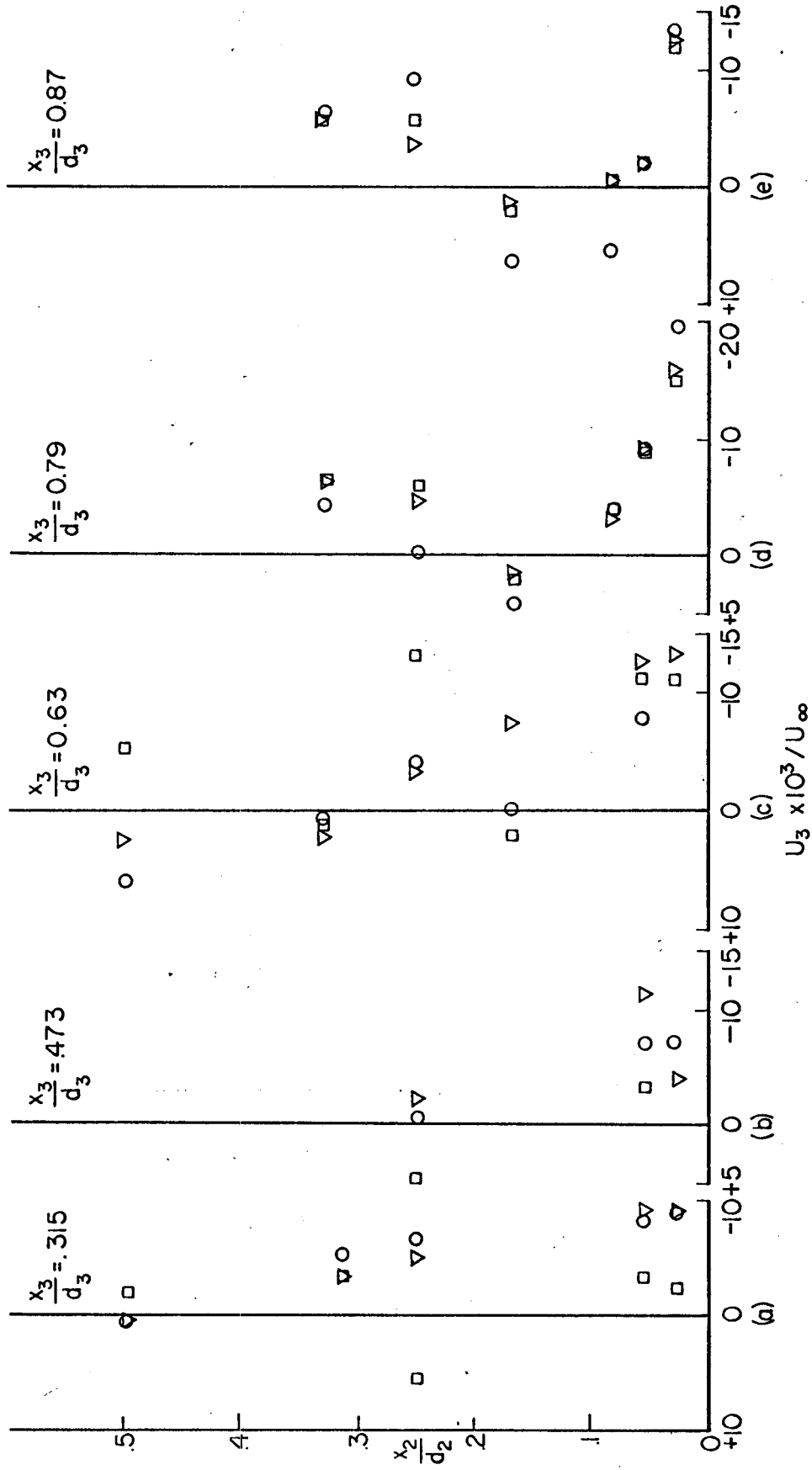


Fig. 6. Horizontal secondary flow components; U_3/U_∞ vs x_2/d_2

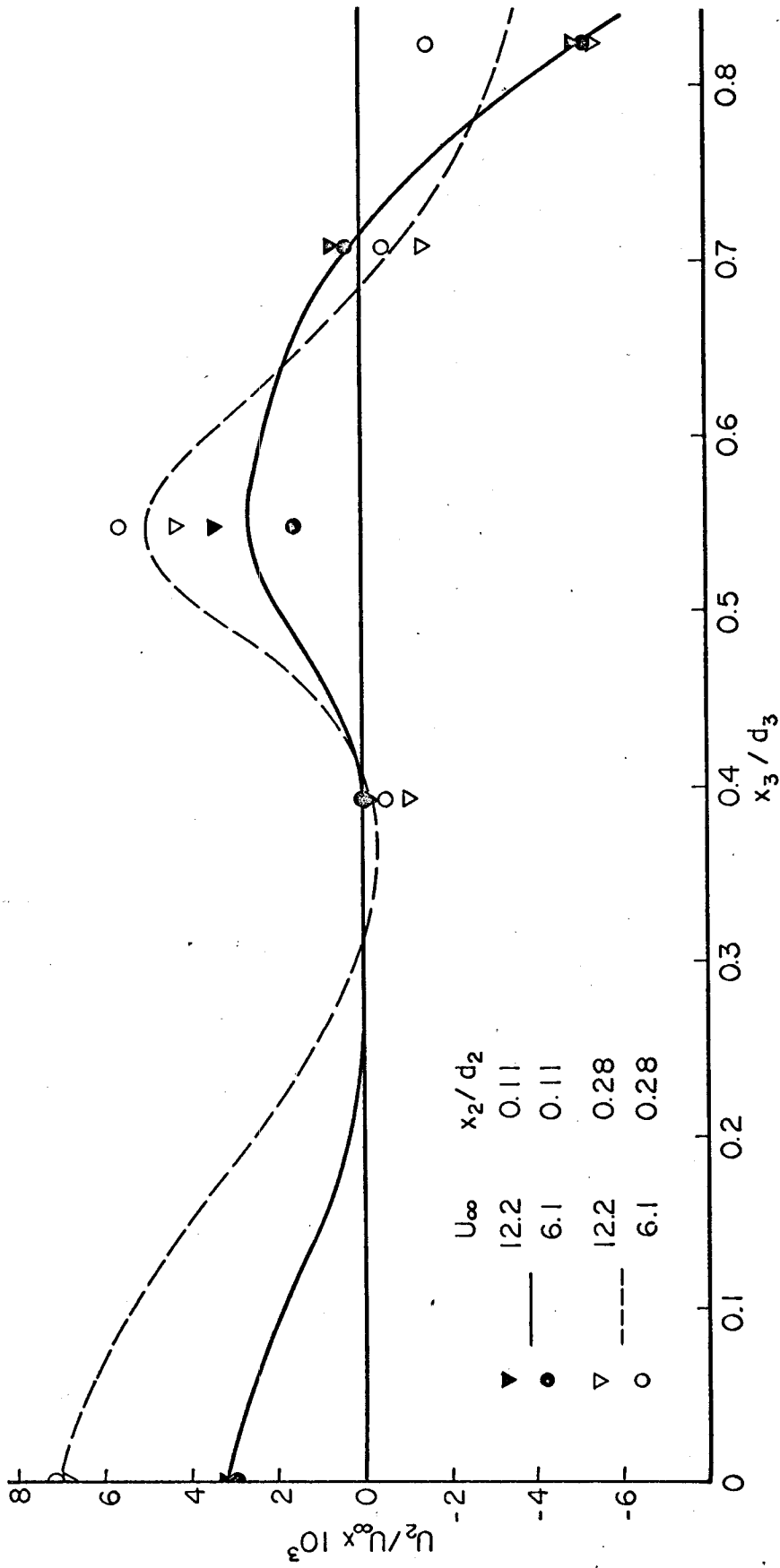


Fig. 7. Calculated vertical secondary flow components; U_2/U_∞ vs x_3/d_3

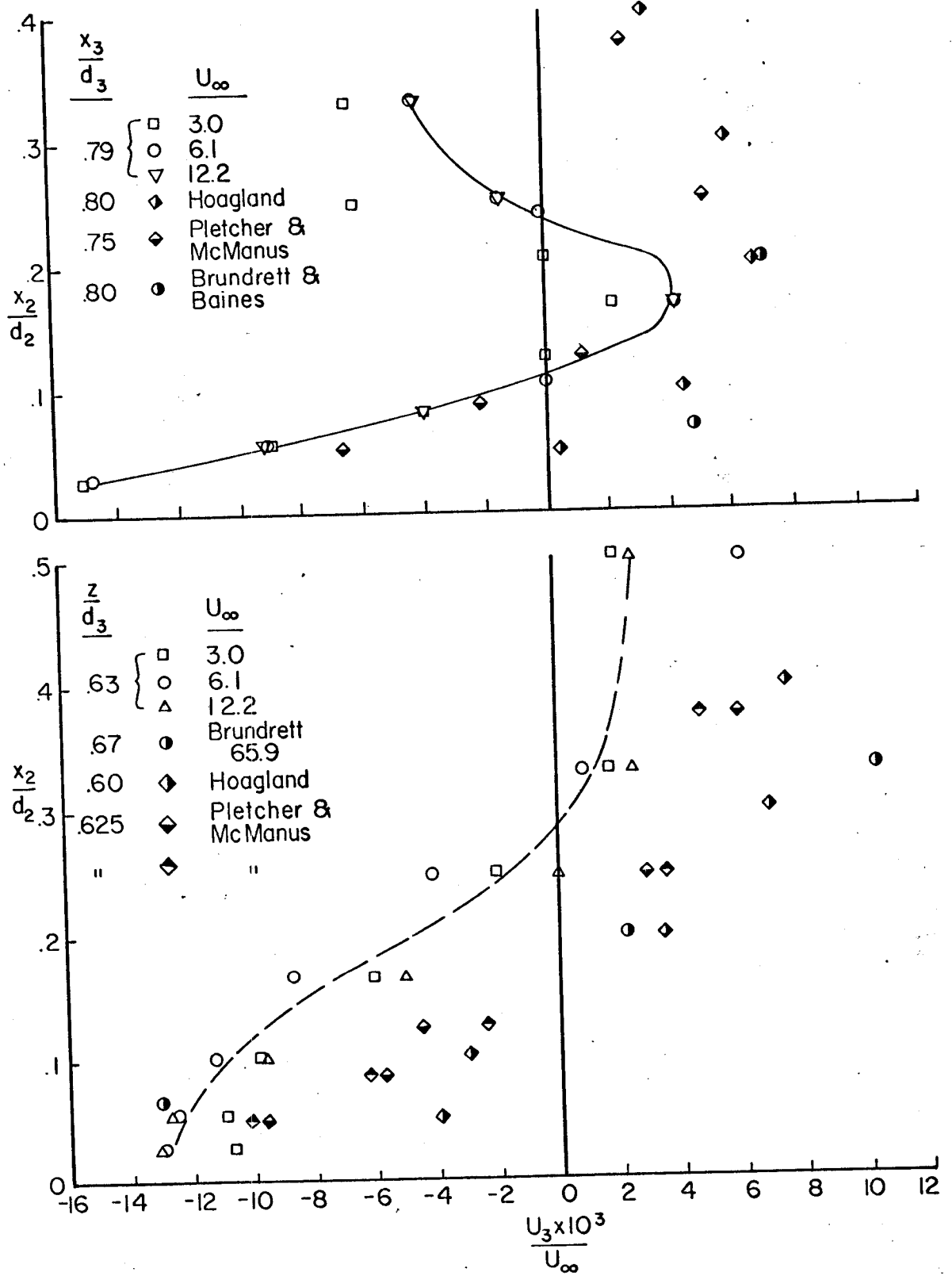


Fig. 8. Comparison with data of other investigators

$$U_{\infty} = 3 \text{ m/s}$$

$$\frac{U_{2,3}}{U_{\infty}} \times 10^3 = 10.0$$

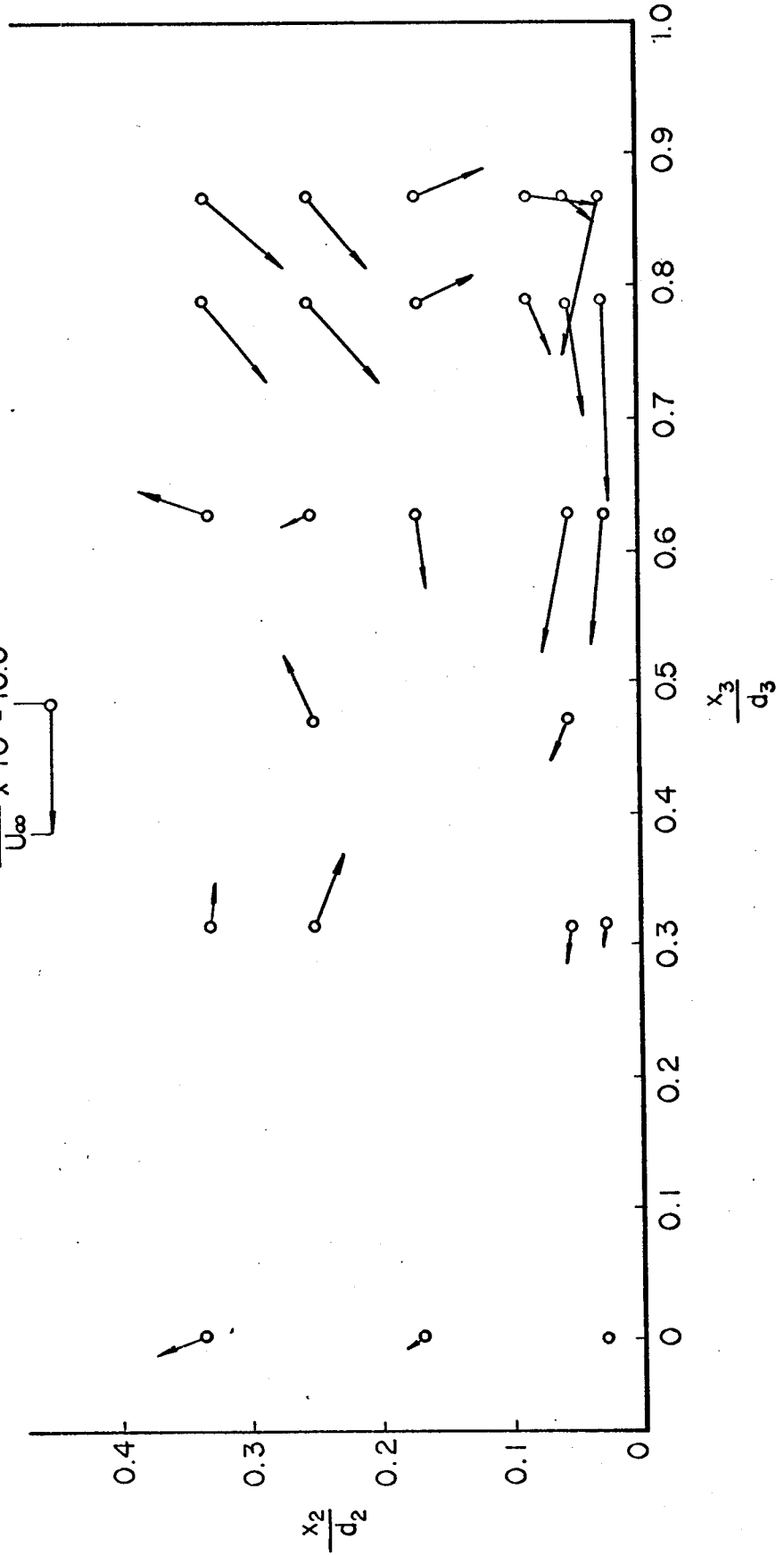


Fig. 9. Resultant secondary flow in cross section, $U_{\infty} = 3 \text{ m/s}$

$$U_\infty = 6.1 \text{ m/s}$$

$$\frac{U_{2,3}}{U_\infty} \times 10^3 = 10.0$$

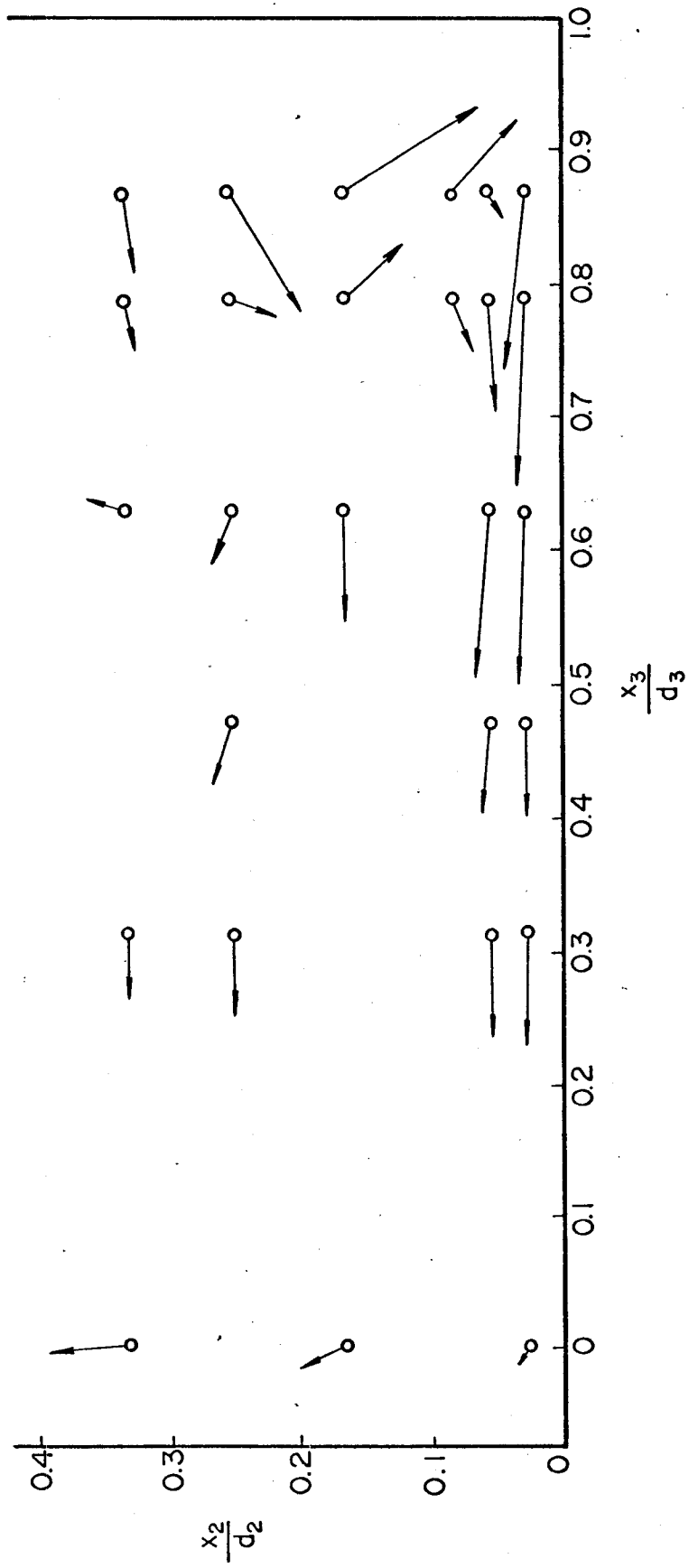
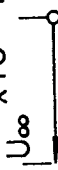


Fig. 10. Resultant secondary flow in cross section, $U_\infty = 6.1 \text{ m/s}$

$$U_{\infty} = 12.2 \text{ m/s}$$

$$\frac{U_{2,3} \times 10^3}{U_{\infty}} = 10.0$$


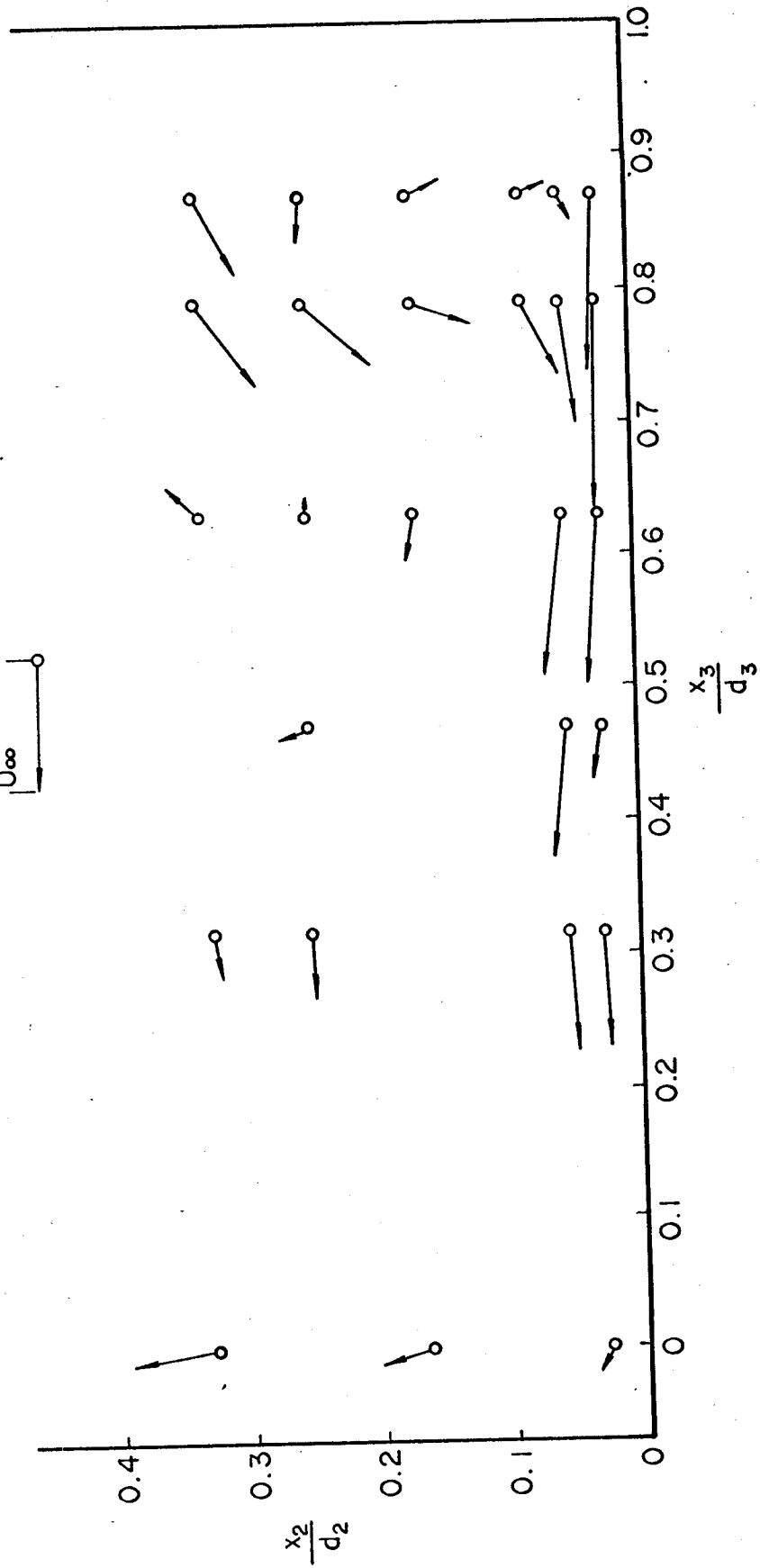


Fig. 11. Resultant secondary flow in cross section, $U_{\infty} = 12.2 \text{ m/s}$

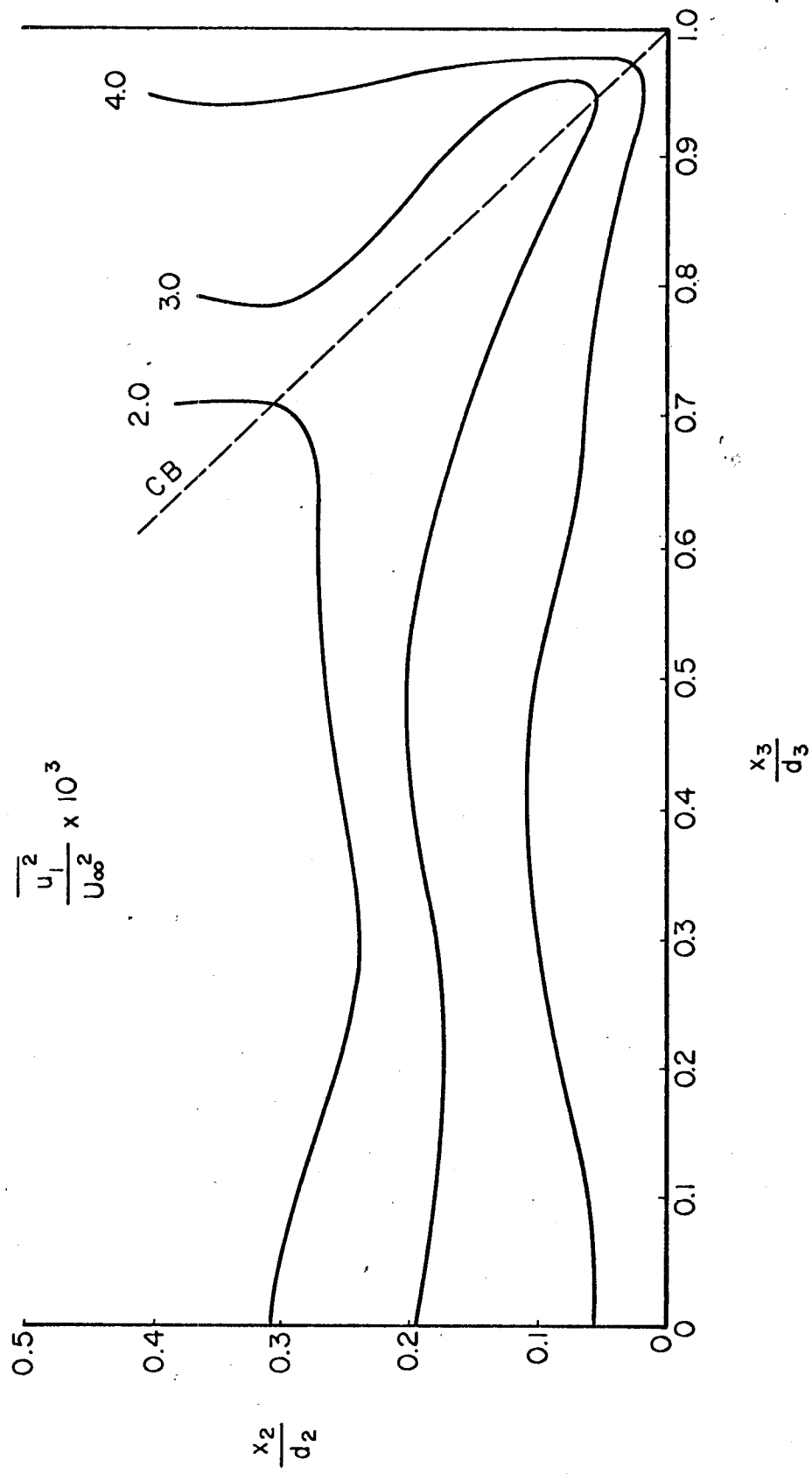


Fig. 12. Distribution of $\overline{u_1^2}/U_\infty^2$

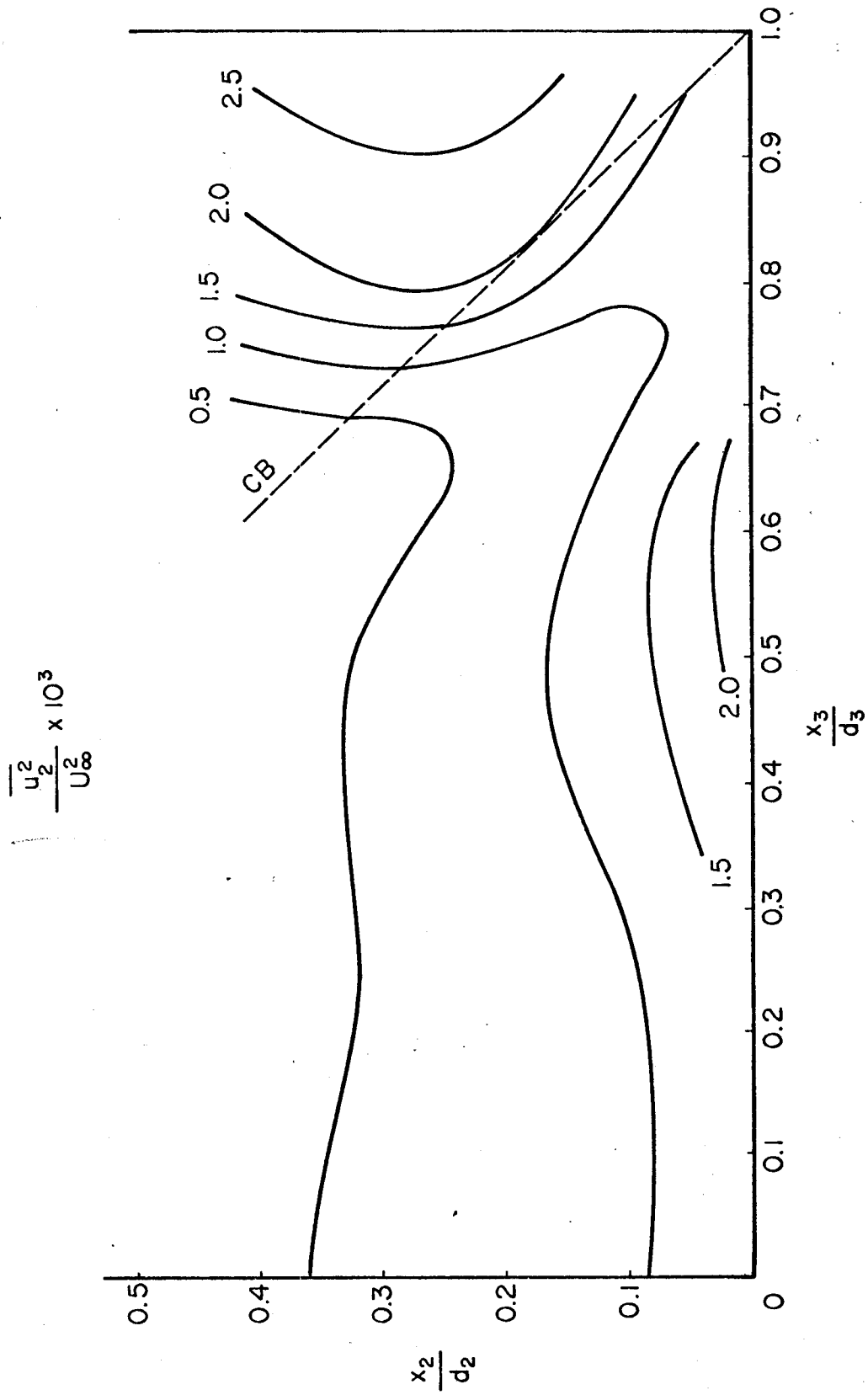


Fig. 13. Distribution of $\overline{u_2^2}/U_\infty^2$

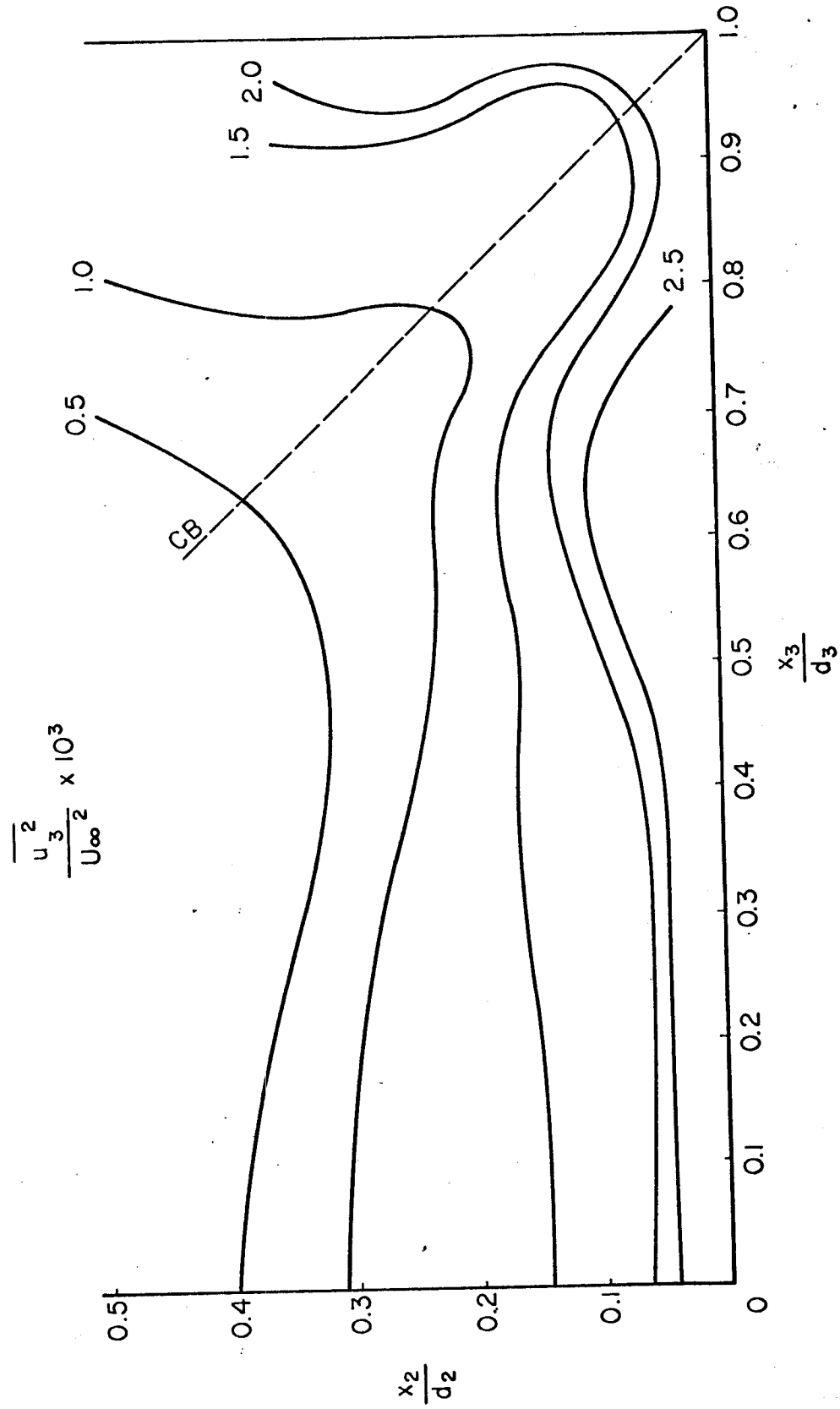


Fig. 14. Distribution of $\frac{\overline{u_3^2}}{U_\infty^2}$

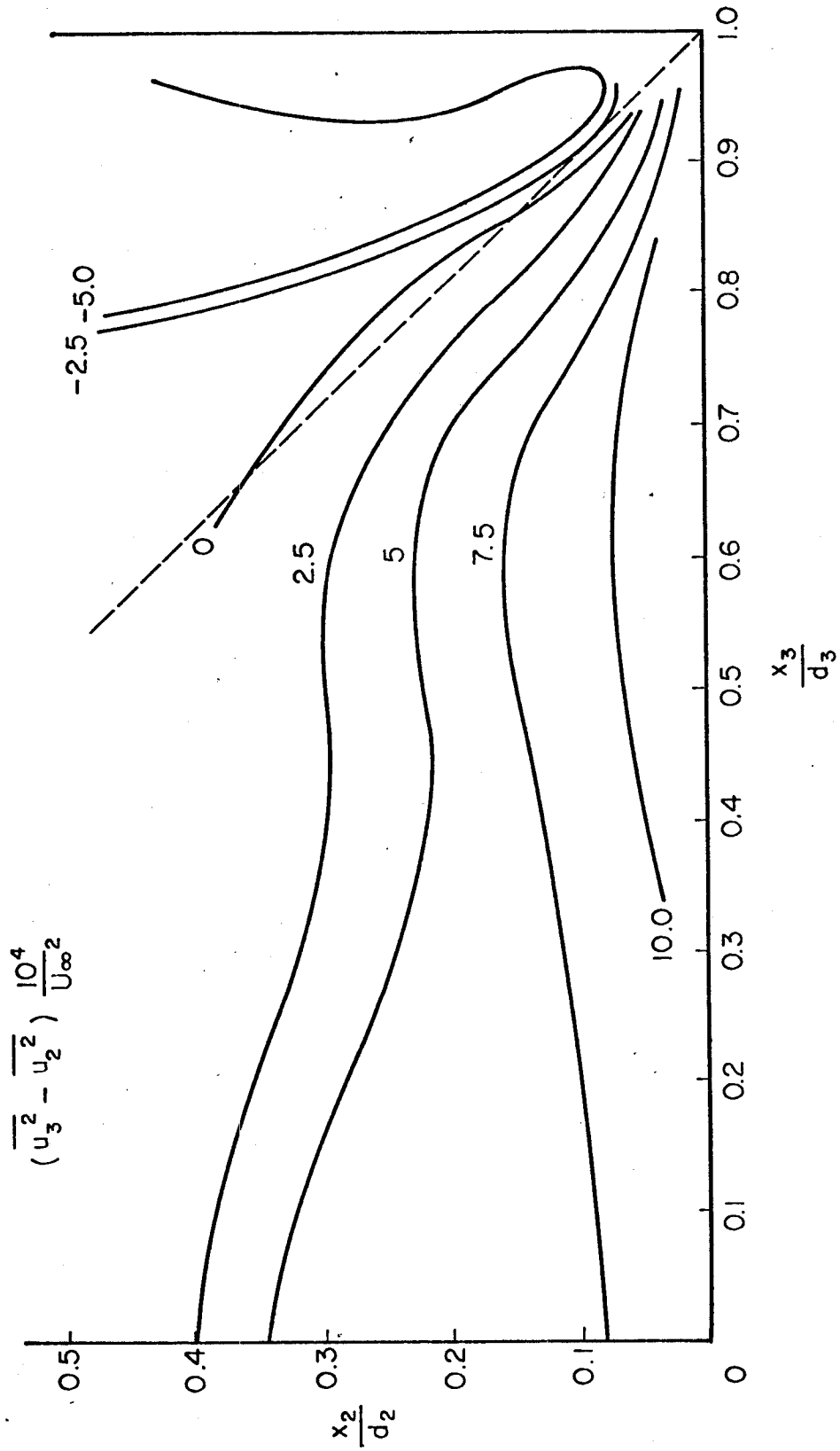


Fig. 15. Distribution of $(u_3^2 - u_2^2) / U_\infty^2$

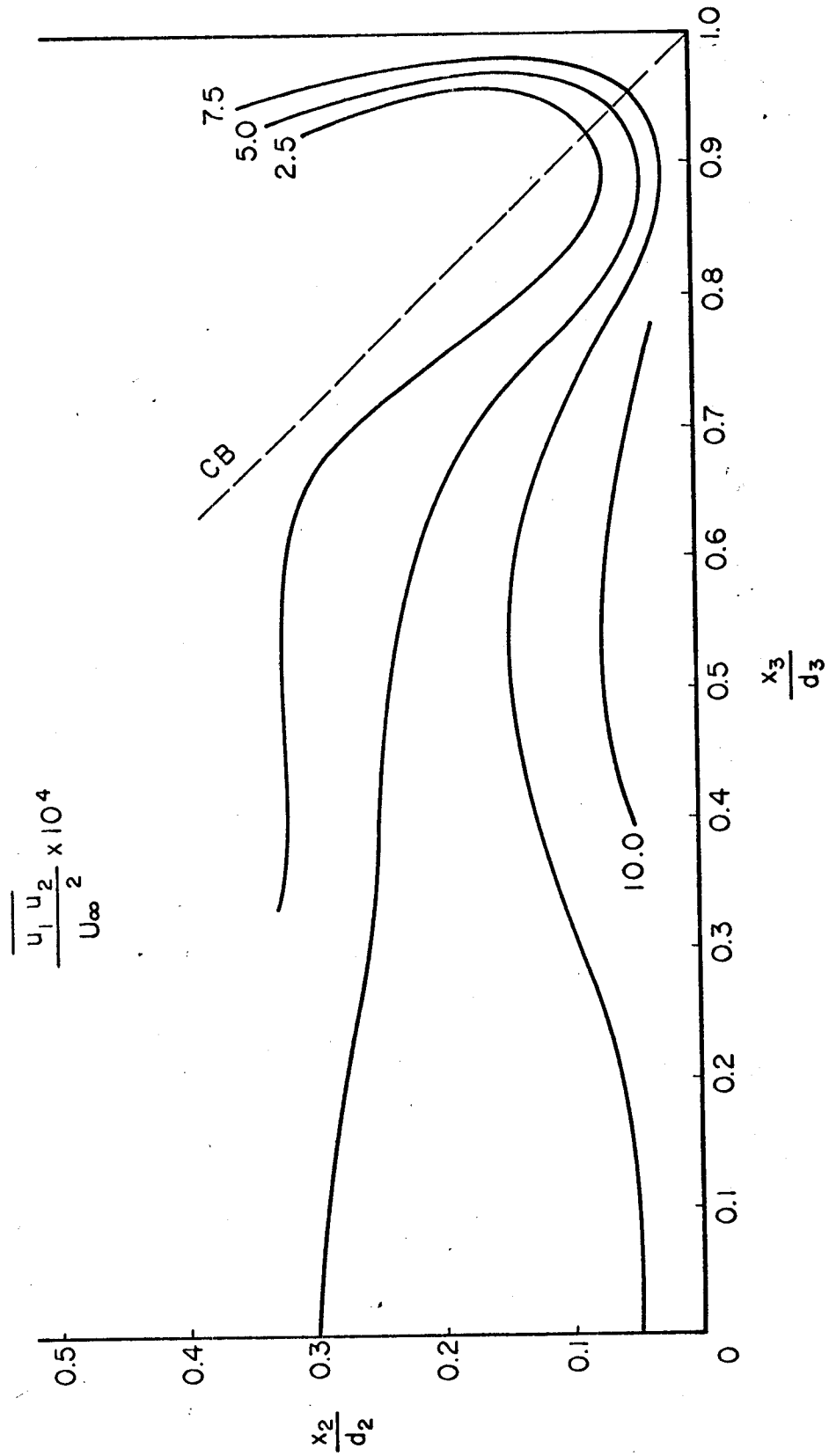


Fig. 16. Distribution of $\overline{u_1 u_2} / U_\infty^2$

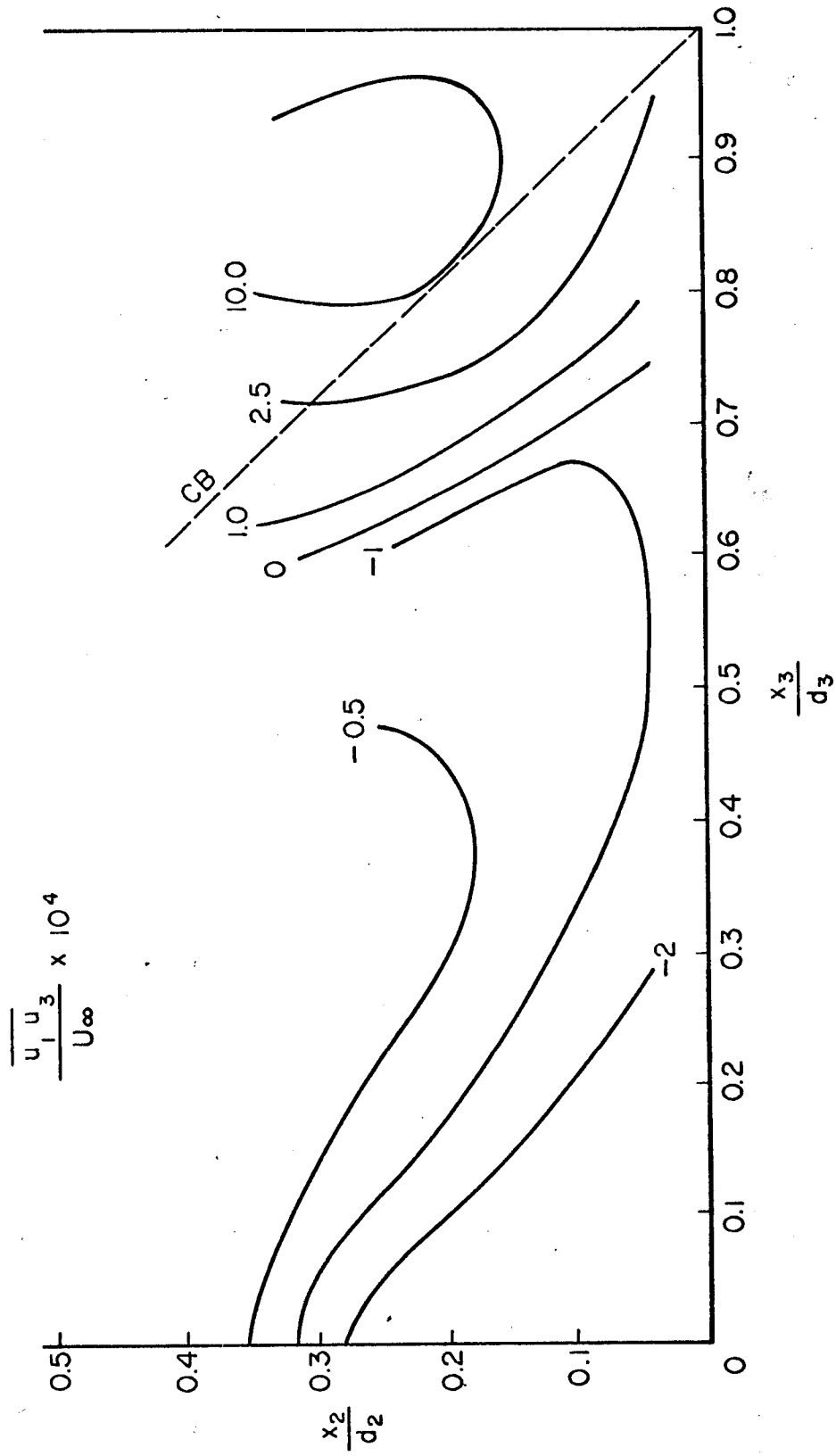


Fig. 17. Distribution of $\overline{u_1 u_3} / U_\infty^2$

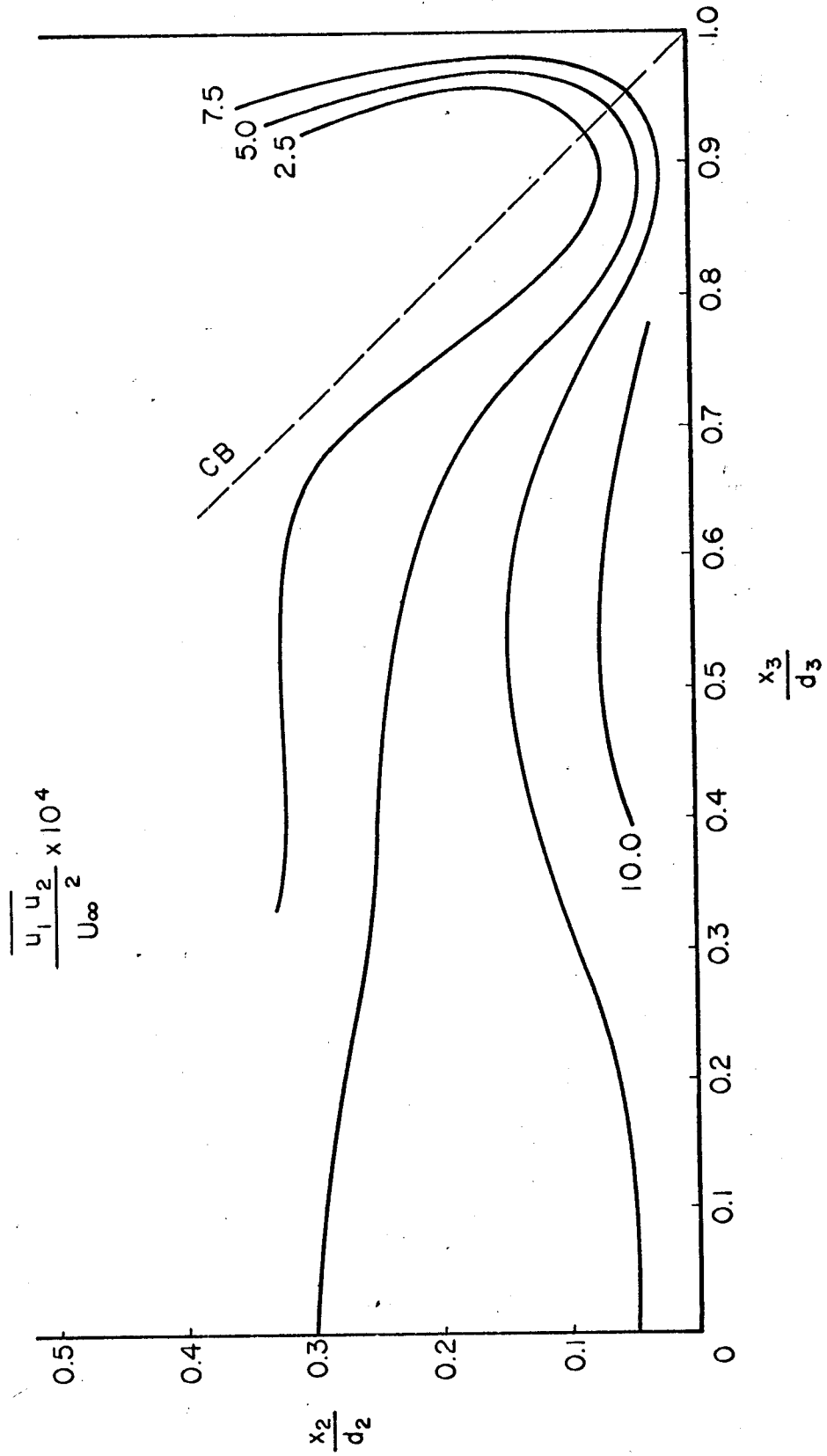


Fig. 16. Distribution of $\overline{u_1 u_2} / U_\infty^2$